Two-spin dephasing by electron-phonon interaction in semiconductor double quantum dots

Xuedong Hu[1]

[1]*Department of Physics, University at Buffalo, SUNY, Buffalo, NY 14260-1500*

(Dated: October 21, 2010)

We study electron-phonon interaction induced decoherence between two-electron singlet and triplet states in a semiconductor double quantum dot using a spin-boson model. We investigate the onset and time evolution of this dephasing, and study its dependence on quantum dot parameters such as dot size and double dot separations, as well as the host materials (GaAs and Si). At the short time limit, electron-phonon interaction only causes an incomplete initial Gaussian decay of the off-diagonal density matrix element in the singlet-triplet Hilbert space. A complete long-time exponential decay due to phonon relaxation would eventually dominate over two-spin decoherence. We analyze two-spin decoherence in both symmetric and biased double quantum dots, identifying their difference in electron-phonon coupling and the relevant consequences.

I. INTRODUCTION

Significant experimental progresses in the study of semiconductor spin qubits in the past few years[1–12] have reconfirmed the confined electron spins as one of the leading candidates for the building block of a solid state quantum information processor. A decade of theoretical studies have mostly clarified single spin decoherence channels and their relative importance in semiconductor quantum dot (QD) and donor confined electrons,[13–32] with hyperfine interaction to the lattice nuclear spins as the main culprit for electron spin decoherence.

Decoherence of two-spin states in a coupled double quantum dot is crucial to the operation and scale-up of exchange-based spin quantum computer architectures.[33–38] Since nuclear spins are the main sources of single spin decoherence in GaAs quantum dots, where most experimental progress have been made, existing theoretical studies have focused on the decohering effects of the nuclear spins.[39–42] In addition, since exchange coupling is electrostatic in nature, exchange-coupled electrons are vulnerable to charge noise and other orbital fluctuations that have an electrical signature.[40,43–47] For example, we have shown how gate noise[43] and background charge fluctuations[44] lead to pure dephasing by introducing noise into exchange splitting of a double dot.

Electron-phonon interaction is intrinsic to any solid state system,[48,49] and semiconductor nanostructures are no exception. It is therefore important to consider the role of electron-phonon interaction in electron spin decoherence. While electron-phonon interaction is generally not spin-dependent, it can affect spins when combined with other interactions. For example, in a single quantum dot, electron-phonon interaction can assist single-electron spin flip or two-spin transitions in combination with spin-orbit interaction[13,19,50–55] or hyperfine interaction.[15,39,42] In the case of donors, the strongly localized electron wave function and the resulting lattice strain lead to a direct spin-lattice interaction, so that electron-phonon interaction can cause pure dephasing for a single spin.[56]

In this work we study decoherence effects of electron-phonon interaction on two-electron-spin states in semiconductor double quantum dots (DQD). Singlet and triplet states are two-spin eigenstates for exchange-coupled electrons in the absence of spin-orbit interaction and inhomogeneous magnetic fields (otherwise electron-phonon interaction can lead to relaxations between singlet and triplet states[42,54,55]). These two types of states have different charge distributions because of their different spin symmetry. We show that this *difference* in electron charge density distribution leads to different dressing by the phonons, without the involvement of the excited states and/or spin-orbit interaction. This difference in phonon dressing then leads to pure dephasing between singlet and triplet states. The systems we consider include coupled quantum dots in GaAs and Si, both regarded as promising candidates for qubits in spin-based quantum information processing.

The paper is organized as follows. In Section II we introduce the electron-phonon interaction in GaAs and Si. Combined with knowledge of two-electron states, we obtain the effective interaction Hamiltonian in the form of a spin-boson model, and calrify the dynamics of two-spin dephasing. In Section III we present our results, quantifying time scale of two-spin dephasing in both GaAs and Si, and in both symmetric and biased double dots, and identifying the most important types of electron-phonon interaction. Finally, in Section IV we discuss the implications of our results on spin and exchange-based quantum information processing, and give our conclusions.

II. THEORETICAL FORMALISM

A. Electron-phonon interaction in GaAs and Si

The general electron-phonon interaction Hamiltonian in a semiconductor takes the form[49]

$$H_{ep} = \sum_{\mathbf{q},\lambda} M_\lambda(\mathbf{q})\rho(\mathbf{q})(a_{\mathbf{q},\lambda} + a^\dagger_{-\mathbf{q},\lambda}), \qquad (1)$$

where $a_{\mathbf{q},\lambda}$ and $a^{\dagger}_{-\mathbf{q},\lambda}$ are phonon annihilation and creation operators with lattice momentum $\mathbf{q}$ and branch index λ, and $\rho(\mathbf{q})$ is the electron density operator. For this work we consider the electron interaction with both acoustic and optical phonons.

For semiconductors with polar characteristics, such as GaAs and InAs, electron-phonon interaction is generally strong, including deformation potential (DP) interaction and piezoelectric (PE) interaction with acoustic phonons, and polar (PO) interaction with longitudinal optical (LO) phonons. Deformation potential interaction in GaAs only couples electrons to longitudinal acoustic (LA) phonons,

$$M^{DP}_{\mathrm{GaAs}}(\mathbf{q}) = D\left(\frac{\hbar}{\rho V\omega_{\mathbf{q}}}\right)^{\frac{1}{2}}|\mathbf{q}|\,, \tag{2}$$

where D is the deformation constant, ρ is the mass density, V is the volume of the crystal, and $\omega_{\mathbf{q}}$ is the angular frequency of the phonon mode $\mathbf{q}$. For GaAs $D = 8.6$ eV and $\rho = 5.3\times10^3$ kg/m^3. For piezoelectric interaction in a zinc-blende lattice,

$$M^{PE}_{\mathrm{GaAs}}(\mathbf{q}) = i\left(\frac{\hbar}{\rho V\omega_{\mathbf{q}}}\right)^{\frac{1}{2}} 2ee_{14}\left(\hat{q}_x\hat{q}_y\xi_z + \hat{q}_y\hat{q}_z\xi_x + \hat{q}_z\hat{q}_x\xi_y\right)\,, \tag{3}$$

where e is the elementary electric charge, e_{14} is an elasticity tensor component, $\hat{\xi}$ is the polarization vector, and $\hat{q}$ is the unit vector along $\mathbf{q}$. For GaAs $e_{14} = 1.38\times10^9$ V/m. Notice that PE interaction can couple electrons to both LA and transverse acoustic (TA) phonons. For polar interaction with LO phonons in bulk polar materials such as GaAs and InAs,

$$M^{PO}_{\mathrm{GaAs}}(\mathbf{q}) = \sqrt{\frac{2\pi e^2\hbar\omega_{LO}}{q^2V}\left(\frac{1}{\epsilon_\infty}-\frac{1}{\epsilon_0}\right)}\,, \tag{4}$$

where ϵ_∞ and ϵ_0 are the high- and low-frequency dielectric constants, and $\hbar\omega_{LO}$ is the zone-center LO phonon energy. For GaAs, $\epsilon_\infty = 10.89$, $\epsilon_0 = 12.9$, and $\hbar\omega_{LO} = 36.25$ meV. In a quantum well with well width a_z, where barrier materials have different dielectric constants than the well itself, the LO phonons are confined, so that the LO phonon wave vectors along the confinement direction can only take discrete values of $q_z = n\pi/a_z$, with n being positive integers.[57]

For Si, which has a vanishing PE interaction because of the inversion symmetry of its lattice, the DP interaction has similar strength as in GaAs, and can couple electrons to both acoustic phonon branches. There is no interaction between conduction electrons and optical phonons in Si though.[49] The conduction band of bulk Si has a six-fold degeneracy at its bottom,[49] so that the DP electron-phonon interaction takes on a more complicated form.[49] For an electron in a particular valley along the $\hat{k}$ direction,

$$H^{DP}_{\mathrm{Si}} = \Xi_d Tr\{\varepsilon\} + \Xi_u(\hat{k}\cdot\varepsilon\cdot\hat{k})\,, \tag{5}$$

where Ξ_d and Ξ_u are the dilation and shear deformation potential constants, and ε is the strain tensor of the lattice due to lattice vibrations. For Si, $\Xi_d = 5.0$ eV and $\Xi_u = 8.77$ eV for electrons at the bottom of the conduction band.[49,58] For a two-dimensional quantum dot (in the xy-plain) whose electronic ground orbital state involves only the z and $-z$ valleys,

$$M^{DP,LA}_{\mathrm{Si}}(\mathbf{q}) = \Xi_d\left(\frac{\hbar}{\rho V\omega_{\mathbf{q}}}\right)^{\frac{1}{2}}|\mathbf{q}|\left(1+\frac{\Xi_u}{\Xi_d}\hat{q}_z^2\right)\,, \tag{6}$$

$$M^{DP,TA}_{\mathrm{Si}}(\mathbf{q}) = \Xi_u\left(\frac{\hbar}{\rho V\omega_{\mathbf{q}}}\right)^{\frac{1}{2}}\xi_z q_z\,. \tag{7}$$

Having obtained the explicit forms of the electron-phonon interaction Hamiltonians in both GaAs and Si, we can now project them onto specific electronic state basis. Below we discuss these projections in both symmetric and biased double quantum dots with two electrons.

B. Charge distribution of two electrons in a symmetric double quantum dot

For two electrons in a DQD, the electron density operator $\rho(\mathbf{q})$ in the general electron-phonon interaction Hamiltonian Eq. (1) takes the form $\rho(\mathbf{q}) = e^{i\mathbf{q}\cdot\mathbf{r}_1} + e^{i\mathbf{q}\cdot\mathbf{r}_2}$.[48] With the knowledge of electron orbital states, we can calculate the matrix elements of $\rho(\mathbf{q})$.

When two spin qubits are exchange-coupled in an unbiased symmetric DQD, their orbital states are symmetric or anti-symmetric if their spin state is singlet ($|\uparrow\downarrow - \downarrow\uparrow\rangle/\sqrt{2}$) or triplet ($|\uparrow\downarrow - \downarrow\uparrow\rangle/\sqrt{2}$, $|\uparrow\uparrow\rangle$, $|\downarrow\downarrow\rangle$). Within the Heitler-London approximation, the two spatial wave functions can be written as

$$\begin{aligned}|\psi_S\rangle &= \frac{1}{\sqrt{2(1+S^2)}}|L(1)R(2)+R(1)L(2)\rangle\,,\\ |\psi_{AS}\rangle &= \frac{1}{\sqrt{2(1-S^2)}}|L(1)R(2)-R(1)L(2)\rangle\,,\end{aligned} \tag{8}$$

where L and R refer to the ground single-electron orbital states in the two dots, $S = \langle L|R\rangle$ is the overlap integral, and 1 and 2 are indices for the two electrons.

Now we can project the electron-phonon interaction into the singlet-triplet Hilbert space. All three triplet states have the same orbital wave function and cannot be differentiated by electron-phonon interaction. The Hilbert space of interest is thus only two-dimensional, with the corresponding basis states $\frac{1}{\sqrt{2(1+S^2)}}|L(1)R(2)+R(1)L(2)\rangle\times\frac{1}{\sqrt{2}}|\uparrow\downarrow - \downarrow\uparrow\rangle$ and $\frac{1}{\sqrt{2(1-S^2)}}|L(1)R(2)-R(1)L(2)\rangle\times\frac{1}{\sqrt{2}}|\uparrow\downarrow + \downarrow\uparrow\rangle$. Since the Hamiltonian has no spin-dependence, the 2×2 electron-phonon interaction Hamiltonian is diagonal:

$$H_{eff} = \sum_{\mathbf{q},\lambda} M_\lambda(\mathbf{q})A_\phi\sigma_z(a_{\mathbf{q},\lambda} + a^{\dagger}_{-\mathbf{q},\lambda})\,, \tag{9}$$

where σ_z is a Pauli matrix in this two-dimensional two-electron Hilbert space (it is not for single electron spins), and the charge distribution difference A_ϕ is given by

$$A_\phi = \frac{1}{2}[\langle\psi_{AS}|\rho(\mathbf{q})|\psi_{AS}\rangle - \langle\psi_S|\rho(\mathbf{q})|\psi_S\rangle] = A_\phi(\mathbf{q}_\parallel) f(q_z)\,. \tag{10}$$

Here $f(q_z)$ is determined by the z-direction (growth direction) wave function, and there is no transition between subbands created by z-confinement. For an infinite square well with width a_z and for acoustic phonons (whose wave vectors are not limited by the quantum well confinement),

$$f(q_z) = \frac{\sin q_z a_z}{q_z a_z} \frac{-\pi^2}{(q_z a_z)^2 - \pi^2}\,. \tag{11}$$

For LO phonons, q_z are discrete: $q_z = m\pi/a_z$, with $m = 1, 2, ...$ In the present calculation there is no intersubband transition, so that

$$f(q_z = 2n\pi/a_z) = 0\,, \tag{12}$$

while for $q_z = (2n+1)\pi/a_z$,

$$f\left(\frac{(2n+1)\pi}{a_z}\right) = \frac{(-1)^{n+1}}{(n-1/2)(n+1/2)(n+3/2)}\,. \tag{13}$$

For a symmetric DQD, the singlet state has larger charge density in between the two dots, while the triplet has larger charge density at the far ends of the DQD. The resulting difference in charge distribution has a finite electrical quadrupole moment and gives $A_\phi(\mathbf{q}_\parallel)$ its $\mathbf{q}$-dependence:

$$A_\phi^{Sym}(\mathbf{q}_\parallel) = \frac{2S^2 e^{-(q_\parallel a)^2/4}}{1-S^4}\left\{\cos q_x L - \cosh\left(\frac{q_y a}{2}\frac{La}{l_B^2}\right)\right\}, \tag{14}$$

where $l_B = \sqrt{\hbar/eB}$ is the magnetic length for a single electron. At zero external field $A_\phi(\mathbf{q}_\parallel)$ takes on the simplified form of

$$A_\phi^{Sym}(\mathbf{q}_\parallel, B=0) = -\frac{4S^2 e^{-(q_\parallel a)^2/4}}{1-S^4}\sin^2\left(\frac{q_x L}{2}\right)\,. \tag{15}$$

C. Charge distribution of two electrons in a biased double quantum dot

In the case of a singlet-triplet qubit,[1] the DQD is biased. The interdot bias is in the regime where the ground triplet state remains in the (11) configuration, while the ground singlet state is generally a superposition of the (11) [denoted as S(11)] and (02) [denoted as S(02)] singlets. In S(11), the two electrons are symmetrically distributed across the two dots. In S(02), the two electrons are both in the ground orbital state of the lower-energy dot. S(11) and S(02) are tunnel coupled, and the composition of the ground singlet state $|\mathrm{S}\rangle$ depends on the detuning ϵ between the two singlets in the absence of the tunnel coupling. Here $\epsilon = 0$ is defined as the anticrossing point of S(11) and S(02). For negative (positive) ϵ, S(11) [S(02)] has lower energy.

$$|\mathrm{S}\rangle = \alpha|\mathrm{S}(11)\rangle + \beta|\mathrm{S}(02)\rangle \tag{16}$$

$$|\mathrm{S}(11)\rangle = \psi_S \times \frac{1}{\sqrt{2}}|\uparrow\downarrow - \downarrow\uparrow\rangle \tag{17}$$

$$|\mathrm{S}(02)\rangle = |R(1)R(2)\rangle \times \frac{1}{\sqrt{2}}|\uparrow\downarrow - \downarrow\uparrow\rangle \tag{18}$$

$$|\mathrm{T}\rangle = \psi_{AS} \times \frac{1}{\sqrt{2}}|\uparrow\downarrow + \downarrow\uparrow\rangle \tag{19}$$

Here for simplicity we assume α and β to be real. Both are functions of the interdot detuning ϵ. With the $|\mathrm{S}\rangle$ and $|\mathrm{T}\rangle$ states given and the respective charge distributions known, we can calculate the charge distribution difference for a biased DQD as a function of α and β:

$$\begin{aligned} A_\phi^{Biased}(\mathbf{q}_\parallel) &= -i\beta^2 e^{-(q_\parallel a)^2/4}\sin q_x L - \alpha\beta\frac{\sqrt{2}S}{\sqrt{1+S^2}} e^{-(q_\parallel a)^2/4}\left\{e^{iq_x L} + \cosh\left(\frac{q_y a}{2}\frac{La}{l_B^2}\right)\right\} \\ &\quad + \left[1 - \frac{\beta^2}{2}(1-S^2)\right]\frac{2S^2}{1-S^4}\, e^{-(q_\parallel a)^2/4}\left\{\cos q_x L - \cosh\left(\frac{q_y a}{2}\frac{La}{l_B^2}\right)\right\} \end{aligned} \tag{20}$$

Similar to the case of a symmetric DQD, at zero magnetic field the expression of A_ϕ is simplified:

$$\begin{aligned} A_\phi^{Biased}(\mathbf{q}_\parallel, B=0) &= -\alpha\beta\frac{2\sqrt{2}S}{\sqrt{1+S^2}}\, e^{-(q_\parallel a)^2/4}\cos^2\frac{q_x L}{2} - \left[1 - \frac{\beta^2}{2}(1-S^2)\right]\frac{4S^2}{1-S^4}\, e^{-(q_\parallel a)^2/4}\sin^2\frac{q_x L}{2} \\ &\quad -i\left[\beta^2 + \alpha\beta\frac{\sqrt{2}S}{\sqrt{1+S^2}}\right] e^{-(q_\parallel a)^2/4}\sin q_x L \end{aligned} \tag{21}$$

The finite interdot bias, which leads to all the additional terms in A_ϕ when $\beta \neq 0$, has some important consequences. One distinct feature of Eq. (21) is the

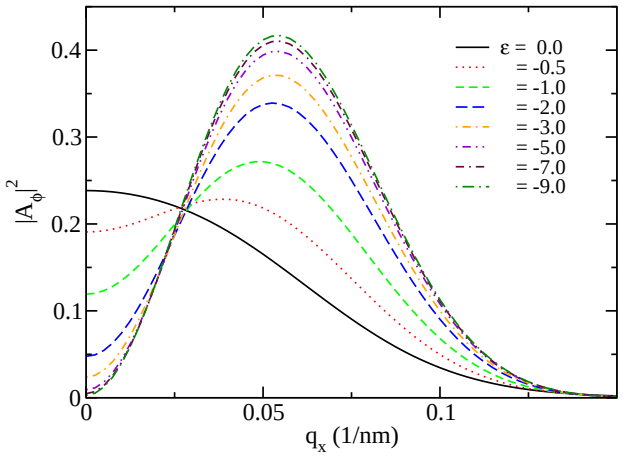

FIG. 1: (Color online) Charge density difference A_ϕ^{Biased} as a function of phonon wave vector q_x and interdot bias ϵ in a biased DQD. Notice that as soon as ϵ moves away from the S(11)-S(02) anticrossing point (where $\epsilon = 0$) toward the negative bias, A_ϕ has similar characteristics in the form of a peak determined by the inter-dot distance L. In this regime the two electrons are in the (11) configuration, essentially the same as the case of a symmetric DQD. Close to $\epsilon = 0$, the two-electron singlet state acquires a (02) component, while the peak of A_ϕ shifts toward $q_x = 0$.

first term on the right hand side, which does not go to zero when $q_x \to 0$. It implies that low-frequency phonons are more efficient in causing dephasing for a biased DQD compared to a symmetric DQD. In Fig. 1 we show A_ϕ^{Biased} as a function of q_x for various detuning ϵ. As discussed above, as ϵ approaches 0, the S(02) component increases in the ground singlet state, and A_ϕ^{Biased} acquires a finite value at $q_x = 0$. On the other hand, for $\epsilon \ll 0$ so that $\beta \to 0$, the biased DQD system approaches the symmetric case, so that $A_\phi^{Biased} \to A_\phi^{Sym}$. Furthermore, for the more symmetric DQDs, A_ϕ has a peak around $q_x \sim 1/L$, as can be seen from the functional form of A_ϕ^{Sym}. Another interesting feature of Eq. (21) is the last term on the right hand side, which apparently does not go to zero when overlap $S \to 0$ as long as β is finite. This term is again due to the charge distribution difference between (11) and (02) configurations. We will explore the consequence of this term at the end of next Section.

D. Two-spin dephasing due to electron-phonon interaction with a dissipative bosonic reservoir

The effective electron-phonon interaction Hamiltonian of Eq. (9) is a typical spin-boson Hamiltonian that leads to decay in the off-diagonal element of the 2×2 density matrix:[59]

$$\rho_{\rm ST}(t) = \rho_{\rm ST}(0) e^{-B^2(t)} , \tag{22}$$

where the dephasing factor is positive definite:[59]

$$B^2(t) = \frac{V}{\pi^3 \hbar^2} \int d^3\mathbf{q} \frac{|M(\mathbf{q}) A_\phi(\mathbf{q})|^2}{\omega_\mathbf{q}^2} \sin^2 \frac{\omega_\mathbf{q} t}{2} \coth \frac{\hbar \omega_\mathbf{q}}{k_B T} . \tag{23}$$

It has long been pointed out that bosonic reservoirs with vanishing density of state at low frequencies do not cause complete decay of the off-diagonal element of a two-level system density matrix,[56,60–68] in other words $B^2(t)$ of Eq. (23) does not diverge with time, because bosonic modes with $\omega \to 0$ determine the long-time behavior for the two-level system. This absence of complete dephasing can be traced back to the assumptions made when the dephasing formula Eq. (23) is derived. While it does account for the fact that the bosonic reservoir is in a thermal equilibrium before getting into contact with the spin,[59] it treats the harmonic modes in the Bosonic reservoir as completely coherent. However, these harmonic modes, in the present case the phonons, also belong to an open system, and could lose their coherence to their environments. When relaxations of the bosonic modes are taken into account, it is expected that pure dephasing of the two-level system would eventually become complete. For example, in a spin-boson model study of localization, Ref. 69 showed how anharmonicity of the bosonic reservoir, in the form of two-phonon scattering, would lead to complete decoherence of the two-level system considered.

In the present study, we account for phonon relaxation by assuming that each phonon mode couples to a continuum of bosonic modes. This is identical to the description of a cavity photon mode coupling to a continuum.[70] Such a model is grounded in the development of phonon cavities in semiconductor heterostructures.[71,72] The Hamiltonian for the phonon modes and their reservoirs takes the form

$$\begin{aligned} H &= H_s + H_r + H_{int} \\ H_s &= \hbar\omega_q a_\mathbf{q}^\dagger a_\mathbf{q} \\ H_r &= \sum_j \hbar\omega_j b_j^\dagger b_j \\ H_{int} &= \hbar \sum_j \left(g_{j\mathbf{q}} a_\mathbf{q}^\dagger b_j + g_{j\mathbf{q}}^* a_\mathbf{q} b_j^\dagger \right) , \end{aligned}$$

where $a_\mathbf{q}$ is the phonon annihilation operator, b_j is the annihilation operator of the jth mode of the bosonic reservoir, and $g_{j\mathbf{q}}$ is the coupling strength between the phonon mode and the reservoir modes. With this interaction with the reservoir, the Langevin equation for the phonon annihilation operator (in the Heisenberg picture) takes the form

$$\begin{aligned} \frac{d}{dt} a_\mathbf{q}(t) &= -i\omega_\mathbf{q} a_\mathbf{q}(t) - \frac{\gamma_\mathbf{q}}{2} a_\mathbf{q}(t) + F_\mathbf{q}(t) e^{-i\omega_\mathbf{q} t} \quad (24) \\ F_\mathbf{q}(t) &= -i \sum_j g_{i\mathbf{q}} b_j(t_0) e^{(\omega_\mathbf{q} - \omega_j)(t - t_0)} \\ \gamma_\mathbf{q} &= 2\pi D(\omega_\mathbf{q}) \left| g(\omega_\mathbf{q}) \right|^2 . \end{aligned}$$

Notice that the noise operator $F_\mathbf{q}(t)$ here is assumed to be independent of the initial time t_0. In the definition

of the decay rate $\gamma_{\mathbf{q}}$ the sum over reservoir mode j has been replaced by an integration over energy, with $D(\omega)$ being the density of state for the reservoir, and g_j is assumed to be smooth in any narrow energy range so that it can be replaced by $g(\omega)$. Compared to a dissipationless phonon mode, now we have the additional 2nd and 3rd terms on the right hand side of Eq. (24), representing the dissipation and fluctuation caused by the coupling to the reservoir. Indeed we expect that whatever the exact form of interaction and spectrum of the reservoir are for the phonons, the effects on the phonons can be characterized by terms similar to these two. We include these two terms and rederive Eq. (23) using the approach adopted in Ref. 59. Now we obtain

$$\rho_{\rm ST}(t) = \rho_{\rm ST}(0) e^{-B_1^2(t) - B_2^2(t)}\,,$$

$$B_1^2(t) = \frac{V}{2\pi^3\hbar^2}\int d^3\mathbf{q} \frac{|M(\mathbf{q})A_\phi(\mathbf{q})|^2}{\omega_{\mathbf{q}}^2 + (\gamma_{\mathbf{q}}/2)^2}\left\{\frac{\omega_{\mathbf{q}}^2 - (\gamma_{\mathbf{q}}/2)^2}{\omega_{\mathbf{q}}^2 + (\gamma_{\mathbf{q}}/2)^2}\left(1 - e^{-\frac{\gamma_{\mathbf{q}}}{2}t}\cos\omega_{\mathbf{q}}t\right) - \frac{e^{-\frac{\gamma_{\mathbf{q}}}{2}t}\omega_{\mathbf{q}}\gamma_{\mathbf{q}}/2}{\omega_{\mathbf{q}}^2 + (\gamma_{\mathbf{q}}/2)^2}\sin\omega_{\mathbf{q}}t\right\}\coth\frac{\hbar\omega_{\mathbf{q}}}{k_BT}\,, \quad (25)$$

$$B_2^2(t) = \frac{V}{2\pi^3\hbar^2}\int d^3\mathbf{q} \frac{|M(\mathbf{q})A_\phi(\mathbf{q})|^2}{\omega_{\mathbf{q}}^2 + (\gamma_{\mathbf{q}}/2)^2}\left(\frac{\gamma_{\mathbf{q}}}{2}t\right) = \Gamma_{\rm ST}t\,. \quad (26)$$

At the limit that phonon decay rate $\gamma_{\mathbf{q}} \to 0$, $B_1^2(t) \to B^2(t)$ while $B_2^2(t) \to 0$. For finite $\gamma_{\mathbf{q}}$, corresponding to a dissipative phonon reservoir, we obtain an additional exponential decay of the off-diagonal density matrix element in Eq. (26) compared to the non-dissipative reservoir result of Eq. (23). The rate of this exponential decay $\Gamma_{\rm ST}$ is proportional to the phonon decay rate $\gamma_{\mathbf{q}}$ integrated over the phonon modes. Notice that $\Gamma_{\rm ST}$ does not explicitly contain the thermal factor $\coth\frac{\hbar\omega_{\mathbf{q}}}{k_BT}$ that describes the thermal occupation of the phonon modes. This is because $B_2^2(t)$ comes from phonons decaying into their reservoirs, when phonons themselves are regarded as coherent bosons, while temperature information of the reservoirs for the phonons is contained in the noise operator $F_{\mathbf{q}}(t)$.

III. RESULTS

The main questions we would like to answer in this work are: Is electron-phonon interaction an important decoherence channel for spin qubits in semiconductor quantum dots? Under what condition is it important? How do different substrate materials (GaAs and Si) compare to each other? And how do different qubit architectures compare with each other? Below we show our results that provide the answers.

A. Symmetric double dot

Let us first examine the dynamical behaviors of the dephasing factors $B^2(t)$ and dephasing rate $\Gamma_{\rm ST}$ due to electron-phonon interaction when the double quantum dot is unbiased.

In Fig. 2 we show the typical behavior of the dephasing factor $B^2(t)$ in the absence of phonon decay for various types of electron-phonon interactions in GaAs and Si. There are two interesting features all the curves for acoustic phonons in Fig. 2 share. At very short times ($t \ll 1$ ps), the increase of $B^2(t)$ is quadratic, which originates from Taylor expansion of the $\sin^2\omega_{\mathbf{q}}t/2$ factor in the integrand at the small-t limit. At long times all the curves saturate, which means that dephasing does not increase with time anymore, so that it corresponds more to a finite loss of contrast than the conventional complete decay of off-diagonal density matrix elements. The transition between the quadratic increase and the saturation happens between 1 and 10 ps for double dots with dot separation of 40 nm and single-dot radius of 20 nm because this time is essentially determined by the interdot distance divided by the speed of sound ($5 \sim 8\times10^3$ m/s in Si and $3 \sim 5\times10^3$ m/s in GaAs): 40 nm / c $\sim$ 10 ps. The saturation time for Si is shorter because Si has larger speed of sound. The dephasing factor due to DP interaction with TA phonons in Si is two orders of magnitude smaller than that due to LA phonons, and is not plotted in Fig. 2.

Mathematically the long-time saturation can be understood by writing $2\sin^2\omega_{\mathbf{q}}t/2$ as $1-\cos\omega_{\mathbf{q}}t = 1-\cos(cqt)$. Since acoustic phonon spectrum is continuous, the cosine term leads to a vanishing contribution to the integral at large times, which leaves the dephasing factor determined by a constant integral that is independent of time. Physically, this saturation is due to the fact that long-time dephasing is determined by the low-frequency part of the spectrum of the bosonic reservoir, while phonon density of state vanishes quadratically at low frequency. In other words, non-dissipative acoustic phonons simply form an inefficient dephasing reservoir as compared to other charge fluctuation reservoirs such as fluctuating charge traps, which have a $1/f$ spectral density. This incomplete dephasing has been observed theoretically in a variety of calculations related to phonons, in the studies of general spin-boson decoherence bahviors, charge and spin coherence of single electrons, and

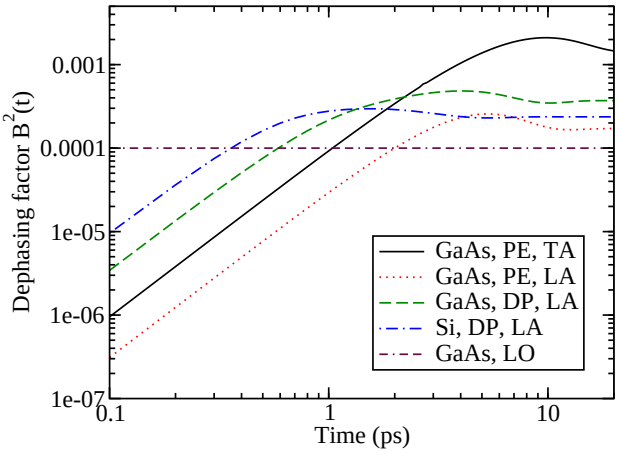

FIG. 2: (Color online) Two-spin dephasing in a symmetric double quantum dot induced by a non-dissipative phonon reservoir. All the curves are for double quantum dots with an interdot separation of 40 nm and single dot orbital radius of 20 nm. More specifically, the black solid line is for PE interaction with TA phonons in GaAs, the red dotted line is for PE coupling to LA phonons in GaAs, the green dashed line is for DP coupling to LA phonons in GaAs; the blue dot-dashed curve is for DP coupling to LA phonons in Si; and the maroon dot-dashed-dashed horizontal line represents the dephasing magnitude for polar interaction with LO phonons in GaAs. The dephasing here is given by $B^2(t\to\infty)$

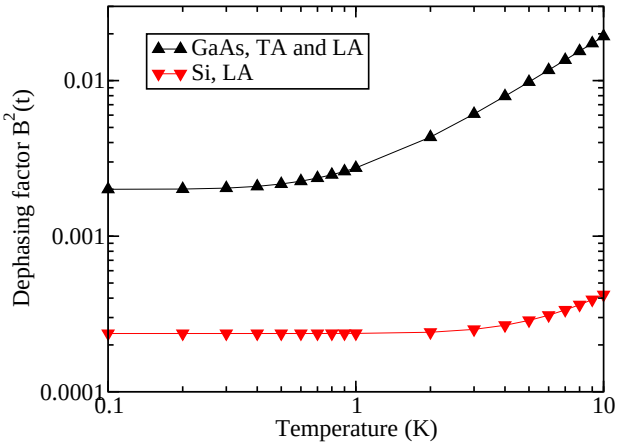

FIG. 3: (Color online) Phonon induced two-spin dephasing rate as a function of acoustic phonon temperature in a symmetric double dot for both GaAs and Si. The single dot wave function radius for all the data is 20 nm.

exciton coherence.[56,60–68]

For electron interaction with optical phonons in GaAs, the dephasing factor $B^2(t)$ takes on a particularly simple form because the optical phonon dispersion at the zone center is flat. Take $\omega_{\mathbf{q}}\approx\omega_{LO}$, we obtain

$$\begin{aligned} B^2_{LO}(t) &= \frac{V}{\pi^3\hbar^2}\int d^3\mathbf{q}\frac{|M(\mathbf{q})A_\phi(\mathbf{q})|^2}{\omega^2_{\mathbf{q}}}\sin^2\frac{\omega_{\mathbf{q}}t}{2}\coth\frac{\hbar\omega_{\mathbf{q}}}{k_BT} \\ &= \frac{2e^2}{\pi^2\hbar\omega_{LO}}\left(\frac{1}{\epsilon_\infty}-\frac{1}{\epsilon_0}\right)\coth\frac{\hbar\omega_{LO}}{k_BT}\sin^2\frac{\omega_{LO}t}{2} \\ &\quad\times\int d^3\mathbf{q}\frac{|A_\phi(\mathbf{q})|^2}{q^2} \\ &= b^2_{LO}\sin^2\frac{\omega_{LO}t}{2}, \end{aligned} \tag{27}$$

which is a sinusoidal function of time. For a GaAs double dot with a single-dot radius of $a=20$ nm, and L/a in the range of 1 and 2, the coefficient b^2_{LO} for the sinusoidal function ranges between 10^{-4} and 10^{-9}.

As we discussed in the previous section, the absolute value of the saturated dephasing, as long as it is small ($\ll 1$), is not an important parameter by itself because dephasing will eventually become complete due to phonon relaxation. However, the relative magnitudes of the saturated dephasing shown in Fig. 2 do give a qualitative sense of the relative importance of various types of electron-acoustic-phonon interactions. Specifically, in GaAs PE coupling to TA phonons produces the strongest dephasing effect, while in Si DP coupling to LA phonons is the most important. In addition, as indicated in Eq.(23), $B^2(t)$ does have a strong temperature dependence as well. At higher temperatures more acoustic phonon modes contribute to dephasing, so that $B^2(t)$ can eventually become an $O(1)$ quantity and dephasing can be considered complete. In Fig. 3 we plot the temperature dependence of the saturated $B^2(t)$ for GaAs and Si quantum dots. At temperatures above 1 K dephasing increases with temperature almost linearly. On the other hand, optical phonon induced dephasing does not have pronounced temperature dependence even at $T=10$ K because $\hbar\omega_{LO}\sim 36$ meV is much larger than k_BT at low temperatures.

When phonon decay is included, the most important effect is the added exponential dephasing $e^{-\Gamma_{\rm ST}t}$, on which we focus in the rest of this study. To calculate $\Gamma_{\rm ST}$, we need to first identify the $\mathbf{q}$-dependence of phonon relaxation rate $\gamma_{\mathbf{q}}$. Qualitatively, lower energy (lower frequency $\omega_{\mathbf{q}}$) acoustic phonons have to decay slower (smaller $\gamma_{\mathbf{q}}$). For example, when phonon decay is due to anharmonicity, or more specifically the 3rd order process of one phonon splitting into two, the phonon decay rate could vary as q^n with n between 1 and 4 depending on the lattice symmetry and phonon branches.[73,74] In the case of a phonon cavity, it is not clear how the Q-factor would vary with phonon wave vector, although with $\gamma_{\mathbf{q}}\propto D(\omega_{\mathbf{q}})$ [where $D(\omega_{\mathbf{q}})$ is the phonon reservoir density of states] one could expect $\gamma_{\mathbf{q}}\propto q^2$. In the following, we calculate acoustic-phonon-induced dephasing rate assuming that $\gamma_{\mathbf{q}}=\gamma_0 q^n$, with n taking the value of 2 or 3. Taking $Q=10^3$ for a TA phonon with energy 0.1 meV, we obtain $\gamma_0=10^8$ 1/s. For LA phonons, which have higher energies than TA phonons with the same q, we take $\gamma_0=10^9$ 1/s. This is an arbitrary choice that is used to reflect the fact that LA phonons generally have shorter lifetimes than TA phonons.[74] For LO phonons we assume a constant relaxation time of 10 ps for all modes.

The rationale here is that LO phonons have a flat dispersion, so that they should have a near constant relaxation rate near the Brillouin zone center. The LO phonons also have a very short lifetime because of their large energy. Zone center LO phonons have been measured to have a lifetime of 7 ps.[75,76]

In Fig. 4 we plot the phonon-induced two-spin dephasing rate $\Gamma_{\rm ST}$ in symmetric DQDs in both GaAs and Si as functions of the half interdot distance L. The radius of the single dot electron wave function is 20 nm for this figure and all the following figures. The strong dependence on L for all data sets originates from the fact that charge distribution difference between the two-electron singlet and triplet states in a symmetric DQD is directly dependent on interdot wave function overlap: $\Gamma_{\rm ST} \propto [4S^2/(1-S^2)]^2$, so that the smaller the overlap, the smaller the difference in charge distribution, and the smaller the phonon-induced dephasing. Based on the data given in Fig. 4, phonon-induced dephasing is not an important decoherence mechanism when $L/a > 2$ in a symmetric DQD.

An important feature of Fig. 4 is that DP coupling to LA phonons is the most important dephasing channel for GaAs, and produces about the same magnitude of dephasing in Si. In GaAs, dephasing due to DP coupling is about one order of magnitude larger than that by PO coupling to LO phonons, and almost two orders of magnitude larger than that due to PE coupling to both LA and TA phonons. This fact is somewhat surprising because in Fig. 2 it is clear that PE coupling to TA phonons is by far the most important decoherence channel. However, notice that in the present calculation of $\Gamma_{\rm ST}$ the acoustic phonon decay increases rapidly as phonon energy increases, so that the contributions from higher-energy phonons are much more important in the calculation of $\Gamma_{\rm ST}$ than in $B^2(t)$. This tilt toward higher-energy phonons strongly favors DP coupling over PE couplings because of the factor of q difference in the electron-phonon coupling matrix element. The similar values for dephasing for GaAs and Si within the DP mechanism is more of a coincidence: they have similar values in DP coupling strength, mass density, and speed of sound, and we chose the same γ_0 for both materials, although Si has the extra contribution from the shear DP constant Ξ_u. Based on the results presented in this figure, phonon-induced dephasing is an essentially equivalent decoherence mechanism for Si and GaAs.

Another interesting aspects of Fig. 4 is that LO phonons turn out to be a strong source of dephasing for the two-spin states in GaAs, even though they have very high energy in GaAs (~ 36 meV). This somewhat surprising result originates from the facts that LO phonons have a diverging density of state at the zone center (as compared to the vanishing density of state for the acoustic phonons) and very fast relaxation rate (experimentally measured at 7 ps[75]), and that GaAs has a reasonably strong polar interaction strength. In Si the conduction electrons do not interact with optical phonons, therefore completely removing this decoherence channel.

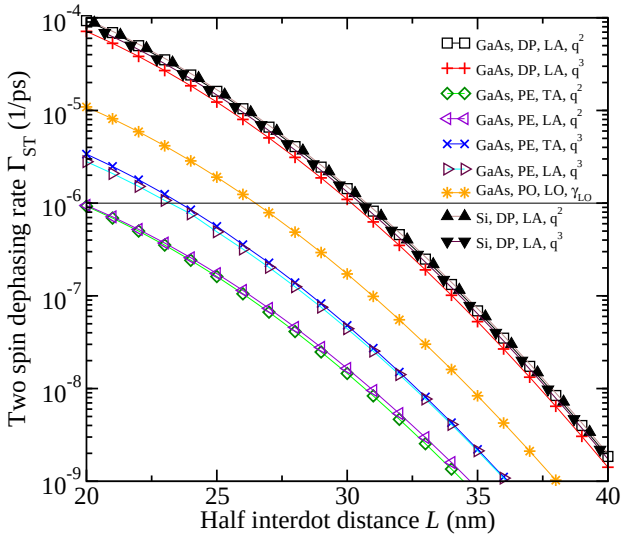

FIG. 4: (Color online) Phonon-induced two-spin dephasing rate as a function of the interdot separation for a GaAs and a Si symmetric double quantum dot. The horizontal line is drawn at a dephasing time of 1 μs, approximately the decoherence times measured in Refs. 1,2. The legends for the data sets have the following format: type of materials (GaAs or Si), type of interaction (DP, PE, or PO), type of phonons involved (LA, TA, or LO), and the q-dependence of $\gamma_{\mathbf{q}}$ (q^2, q^3, or constant γ_{LO}).

For DP and PE interactions the different q-dependence of phonon relaxation rate $\gamma_{\mathbf{q}}$ leads to quite different results in two-spin dephasing rate $\Gamma_{\rm ST}$. With DP interaction, $\Gamma_{\rm ST}$ is not very sensitive to the exponent n, and increasing n in $\gamma_{\mathbf{q}} \sim q^n$ leads to a slight decrease of $\Gamma_{\rm ST}$. On the other hand, for PE interaction, increasing n leads to an approximately three-fold increase of $\Gamma_{\rm ST}$. The change of the exponent n leads to a shift of the dominant $\mathbf{q}$ region that contributes to dephasing. For PE interaction, increasing n from 2 to 3 moves the dominant contribution to larger q phonons, which have larger density of states, leading to an increase in $\Gamma_{\rm ST}$. For DP interaction, the dominant contribution already comes from the $qa \sim 1$ region, where changing n does not have much of an effect.

In Fig. 5 we plot the two-spin merit figure $\mathcal{M}$ as a function of the interdot distance for double dots in GaAs. Here the merit figure is defined as the ratio between a typical exchange gate time given by $\hbar/J$ (J is the exchange splitting) and the two-spin decay time given by $1/\Gamma_{\rm ST}$: $\mathcal{M} = J/\hbar\Gamma_{\rm ST}$. The exchange splitting J is calculated within the Heitler-London model with a quartic confinement potential[77]. The increase of the merit figure at larger inter-dot distance reflects the fact that the exchange splitting and the phonon-induced dephasing have different dependence on the interdot overlap integral S: $J \sim S^2$, while $\Gamma_{\rm ST} \sim S^4$. The results shown in this figure indicate that for a two-dot exchange gate to oper-

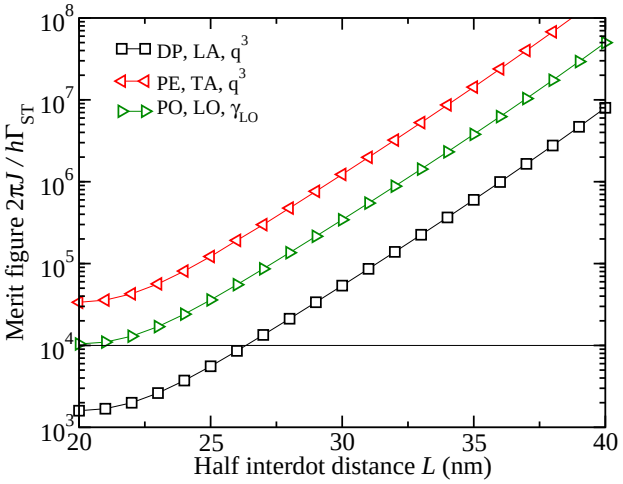

FIG. 5: (Color online) Merit figure based on phonon-induced dephasing of two-spin states in a symmetric GaAs double dot as a function of half interdot distance. We draw a line at 10^4 as the nominal threshold for fault tolerant quantum computation. Therefore the double dot (with single-dot wave function radius at 20 nm) should be kept apart further than 60 nm. The legend format is similar to in Fig. 4 (without the first item for materials as all data here are for GaAs): type of coupling, type of phonon, and q-dependence of $\gamma_{\mathbf{q}}$.

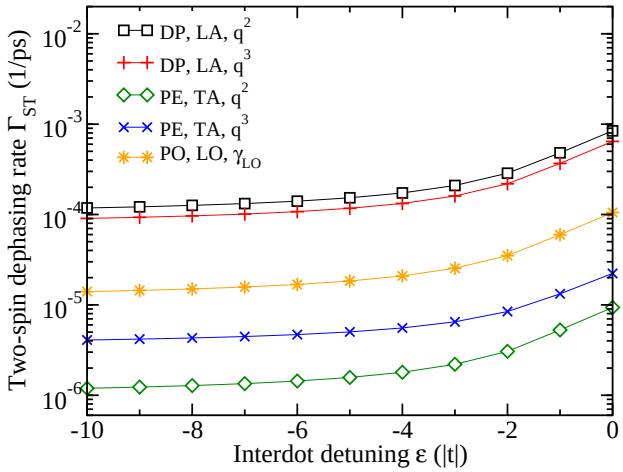

FIG. 6: (Color online) Phonon-induced two-spin dephasing rate as a function of the interdot bias ϵ for a GaAs double quantum dot with piezoelectric coupling to transverse phonons. The double dot are separated by 40 nm and the single-dot wave function radius is 20 nm, so that we are at the strong coupling limit. At large negative bias the relaxation rate approaches a value of about 10^{-6} 1/ps, or T_ϕ of about 1 μs. As the bias increases toward the S(11)-S(02) anticrossing, the dephasing rate increases so that at $\epsilon = 0$, $T_\psi \sim 100$ns.

ate with a low error rate, slower operation with smaller interdot overlap is preferable with regard to phonon-induced dephasing, and fault-tolerant two-qubit operations should be achievable for pretty strongly coupled dots, with $L/a \gtrsim 1.5$. We do not have any data for Si DQDs in this figure. Calculating exchange interaction in a Si double dot requires much more sophisticated quantum chemical approaches than a simple Heitler-London approximation[43,78,79] because in Si the interaction effect is stronger compared to GaAs (larger effective mass and smaller dielectric constant), so that Heitler-London approximation does not adequately account for the two-electron correlation. For the current evaluation, it is sufficient to point out that Fig. 4 above indicates that phonon-induced dephasing is about the same order of magnitude in Si as in GaAs, while exchange coupling should only be somewhat smaller than in GaAs. Therefore overall the merit figure should remain about the same when moving from GaAs to Si.

B. Biased double dot

For a biased DQD, the main question is whether the admixture from S(02) singlet state and the resulting dipole coupling would lead to significantly increased dephasing. Interestingly, the bias not only directly affects the value of $A_\phi(\mathbf{q}_\parallel)$, but also its functional form. In Fig. 1 we have shown how $A_\phi(q_x, q_y = 0)$ depends on q_x for various interdot bias ϵ. It is clear from that figure that the peak of A_ϕ shifts toward $q_x = 0$, while the peak height decreases, as the interdot bias shifts from (11) toward (02) regime. Furthermore, Eq. (21) indicates that as soon as $\beta \neq 0$, there is a mixing of S(11) and S(02) states, so that A_ϕ^{Biased} acquires a nonvanishing component [1st term on the right hand side of Eq. (21)] as $q_x \to 0$, leading to an increase in the phonon-induced dephasing.

Now we can calculate the two-spin dephasing rate $\Gamma_{\rm ST}$ for any voltage bias between the dots. Figure 6 shows $\Gamma_{\rm ST}$ as a function of dimensionless interdot bias ϵ. As ϵ becomes increasingly negative, the biased DQD states approach those of a symmetric DQD, and $\Gamma_{\rm ST}$ approaches the value given in Fig. 4. On the other hand, as ϵ increases toward positive bias, the ground singlet state has a larger S(02) component, and A_ϕ a larger dipolar contribution, so that $\Gamma_{\rm ST}$ increases. At $\epsilon = 0$, $\Gamma_{\rm ST}$ is dominated by the dipolar contribution from the S(11)-S(02) mixing, and is about ten times larger than in a symmetric DQD, where A_ϕ is determined by a quadrupolar charge distribution difference between S(11) singlet and T(11) triplet states.

As indicated in Fig. 4, for symmetric DQDs phonon-induced decoherence becomes much less important at larger L because of the overlap factor S in the charge difference A_ϕ. In the case of a biased DQD, when the DQD has a vanishing overlap,

$$A_\phi^{Biased}(B = 0, S = 0) = -i\beta^2 e^{-(q_\parallel a)^2/4} \sin q_x L\,, \quad (28)$$

which does not seem to depend on the interdot overlap. This term originates from dephasing between T(11) and S(02) states, which clearly have different charge distributions. However, if S vanishes because the interdot

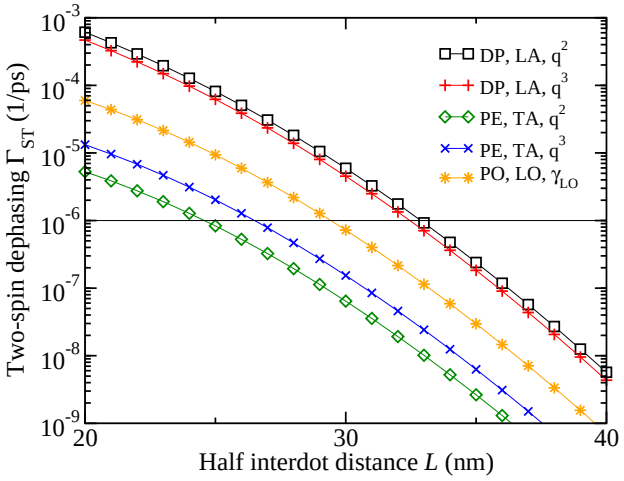

FIG. 7: (Color online) Phonon-induced two-spin dephasing rate as a function of the interdot distance L for a biased GaAs double quantum dot with DP coupling to LA phonons, PO coupling to LO phonons, and PE coupling to TA phonons. The format of the legend is the type of coupling, the type of phonon, and the q-dependence of the phonon relaxation rate $\gamma_{\mathbf{q}}$. The single-dot wave function radius is 20 nm, and the interdot bias is $\epsilon = -1$ at $L = 20$ nm.

distance L increases, phonon-induced dephasing will not saturate to a constant, as Eq. (28) seems to indicate, because β depends on L as well. Recall that the tunnel coupling t of the S(11) and S(02) singlet states is $t = \langle \mathrm{S}(11)|H|\mathrm{S}(02)\rangle \propto S = e^{-L^2/a^2}$. When L increases, t decreases as $t = t_0\, e^{-(L^2-L_0^2)/a^2}$ for two coupled parabolic dots, where t_0 is the tunnel coupling at L_0. For a fixed interdot bias ϵ [Recall that $\epsilon = 0$ corresponds to the S(11)-S(02) crossing point, where $\beta^2 = 0.5$], the DQD moves further from the anticrossing point as t gets smaller, leading to a decreasing β [which is the weight of the higher-energy singlet. For negative ϵ it is the weight of S(02) state]. In Fig. 7 we plot the dephasing rate for a biased DQD as a function of the interdot separation. The figure shows the same rapid decrease of dephasing for all types of phonons as L increases, similar to the situation in symmetric DQDs. Indeed, putting $\beta \propto S$ into Eq. (21), it is clear that $A_\phi^{biased} \propto S^2$, which is the same overlap-dependence as in the case of a symmetric DQD.

The results in Figs. 6 and 7 show that in a biased DQD phonon-induced dephasing approaches symmetric DQD limit at large negative bias, and increases monotonically as interdot bias ϵ increases. However, one can always reduce this dephasing by increasing interdot distance and reducing wave function overlap. Furthermore, for larger negative biases [deeper into the (11) regime, with smaller exchange splitting $J = t/2\epsilon$], β^2 is smaller. When $|\epsilon| \gg 1$, $\beta^2 \sim (1/\epsilon)^2$ while $J \propto 1/\epsilon$. Therefore there should exist a regime where dephasing rate Γ_{ST} is much smaller than exchange splitting, so that fault-tolerant exchange gates can be performed. For example, if we choose $L/a = 2$ with $a = 20$ nm, $1/\Gamma_{\mathrm{ST}} \sim 100$ μs even at $\epsilon = -1$, according to Fig. 7. At such an interdot separation, $|t| \sim 10\mu$eV, so that $J \sim 1$ μeV for $\epsilon = -10$, with a gate time in the order of a nanosecond, leading to a merit figure of $\sim 10^5$.

IV. DISCUSSIONS AND CONCLUSIONS

Based on our results presented in this study, phonon induced two-spin dephasing in both symmetric DQDs and biased DQDs can be strongly suppressed by reducing the double dot tunnel coupling. The strong overlap dependence of the dephasing rate dictates that phonon-induced dephasing is only important when the double dot is tightly coupled. Dephasing for a biased double dot does increase with bias because of the admixture of S(02) state in the singlet ground state, which introduces electric dipole coupling into phonon-induced decoherence. Therefore, phonon-induced two-spin dephasing is generally stronger in biased DQDs, such as in the case of a singlet-triplet qubit.

Phonon induced two-spin dephasing studied in this paper is related to the different dressing that singlet and triplet electronic states experience through interaction with the phonons. When phonons themselves decohere, this spin dephasing channel leads to true complete decoherence. On the other hand, ensemble average over phonon modes (while each evolve coherently) only leads to a finite degree of dephasing. A legitimate question here is whether this part of the dephasing (due to phonon population average) would disappear if we consider dressed electron spin states, especially considering that this finite dephasing generally saturates in the order of 10 ps, much faster then the electron spin initialization and manipulation processes in quantum dots. Mathematically, the answer to this question may very well be "yes", as long as one can identify the energies of the dressed states precisely. But to answer this question with confidence, one needs to clarify how the energies of the spin states are measured, and how electron-phonon interaction may be incorporated in the description of measurement. In the current generation devices spin detection is achieved through charge sensing in the spin-blockade regime,[80] which is insensitive to phonons, so that the phonon-induced dephasing due to ensemble averaging cannot be removed. Ultimately, though, this question is moot because phonons do relax and are not coherent forever.

The phonon-induced pure dephasing mechanism we consider here originates from the charge distribution difference between states that have different spatial symmetry, and involves no real or virtual phonon emission or absorption. It is different from another mechanism of phonon-induced dephasing studied in Ref. 46, which is based on different level distribution of electron singlet and triplet states and involves virtual emission and absorption of phonons.

In conclusion, we have studied phonon-induced pure dephasing between two-electron singlet and triplet spin

states in a semiconductor double quantum dot. We find that this pure dephasing is important for tightly coupled double dots, but is strongly suppressed when the double dot separation increases, so that at relatively large dot separations ($L/a > 2$) fault-tolerant exchange gates can be realized. A biased double dot has stronger dephasing compared to a symmetric double dot with the same dot parameters due to the mixing of (11) and (02) singlet states and the resulting finite electric-dipole coupling. We have quantified two-spin dephasing in both GaAs and Si double dots, finding that deformation potential coupling to LA phonons is the most important dephasing mechanism in both materials, and produces about the same magnitude dephasing in both materials. We also find that LO-phonon makes a non-negligible contribution to dephasing in GaAs because of the very fast optical phonon relaxation. Overall, phonon-induced two-spin dephasing is an equivalent decoherence mechanism for Si and GaAs, is stronger in a biased double dot than in a symmetric double dot, and can be suppressed by reducing the interdot overlap of the electron wave functions.

This work is supported by NSA and LPS through ARO. We also thank the hospitality and financial support of Joint Quantum Institute at the University of Maryland and Kavli Institute of Theoretical Physics at the University of California at Santa Barbara, where part of this work was performed. We have benefited greatly from useful discussions with Peter Yu, Luming Duan, Hendrik Bluhm, Sankar Das Sarma, Guy Ramon, and Susan Coppersmith.

[1] J.R. Petta, A.C. Johnson, J.M. Taylor, E.A. Laird, A. Yacoby, M.D. Lukin, C.M. Marcus, M.P. Hanson, and A.C. Gossard, Science **309**, 2180 (2005).
[2] F.H.L. Koppens, K.C. Nowack, and L.M.K. Vandersypen, Phys. Rev. Lett. **100**, 236802 (2008).
[3] N. Shaji, C.B. Simmons, L.J. Klein, H. Qin, D.E. Savage, M.G. Lagally, S.N. Coppersmith, R. Joynt, M. Friesen, R.H. Blick, and M.A. Eriksson, Nature Physics **4**, 540 (2008).
[4] G.P. Lansbergen, R. Rahman, C.J. Wellard, I. Woo, J. Caro, N. Collaert, S. Biesemans, G. Klimeck, L.C.L. Hollenberg, and S. Rogge, Nature Physics **4**, 656 (2008).
[5] M. Pioro-Ladriere, T. Obata, Y. Tokura, Y.S. Shin, T. Kubo, K. Yoshida, T. Taniyama, and S. Tarucha, Nature Phys. **4**, 776 (2008).
[6] I.T. Vink, K.C. Nowack, F.H.L. Koppens, J. Danon, Y.V. Nazarov, and L.M.K. Vandersypen, Nature Phys. **5**, 764 (2009).
[7] Y.S. Shin, T. Obata, Y. Tokura, M. Pioro-Ladriere, R. Brunner, T. Kubo, K. Yoshida, and S. Tarucha, Phys. Rev. Lett. **104**, 046802 (2010).
[8] J.R. Petta, H. Lu, and A.C. Gossard, Science **327**, 669 (2010).
[9] M. Xiao, M.G. House, and H.W. Jiang, Phys. Rev. Lett. **104**, 096801 (2010).
[10] D.J. Reilly, J.M. Taylor, J.R. Petta, C.M. Marcus, M.P. Hanson, and A.C. Gossard, Phys. Rev. Lett. **104**, 236802 (2010).
[11] S. Foletti, H. Bluhm, D. Mahalu, V. Umansky, and A. Yacoby, Nature Phys. **5**, 903 (2009).
[12] H. Bluhm, S. Foletti, I. Neder, M. Rudner, D. Mahalu, V. Umansky, and A. Yacoby, `arXiv:1005.2995`.
[13] A.V. Khaetskii and Yu.V. Nazarov, Phys. Rev. B **64**, 125316 (2001).
[14] I.A. Merkulov, A.L. Efros, and M. Rosen, Phys. Rev. B **65**, 205309 (2002).
[15] S.I. Erlingsson and Yu.V. Nazarov, Phys. Rev. B **66**, 155327 (2002).
[16] C. Tahan, M. Friesen, and R. Joynt, Phys. Rev. B **66**, 035314 (2002).
[17] A.V. Khaetskii, D. Loss, and L. Glazman, Phys. Rev. Lett. **88**, 186802 (2002).
[18] W.A. Coish and D. Loss, Phys. Rev B **70**, 195340 (2004).
[19] V.N. Golovach, A.V. Khaetskii, and D. Loss, Phys. Rev. Lett. **93**, 016601 (2004).
[20] R. de Sousa and S. Das Sarma, Phys. Rev. B **67**, 033301 (2003).
[21] R. de Sousa and S. Das Sarma, Phys. Rev. B **68**, 115322 (2003).
[22] W.M. Witzel, R. de Sousa, and S. Das Sarma, Phys. Rev. B **72**, 161306R (2005).
[23] W.M. Witzel and S. Das Sarma, Phys. Rev. B **74**, 035322 (2006).
[24] W. Yao, R.B. Liu, and L.J. Sham, Phys. Rev. B **74**, 195301 (2006).
[25] R.B. Liu, W. Yao, and L.J. Sham, New J. Phys. **9**, 226 (2007).
[26] C. Deng and X. Hu, Phys. Rev. B **73**, 241303 (2006).
[27] W.M. Witzel, X. Hu, and S. Das Sarma, Phys. Rev. B **76**, 035212 (2007).
[28] C. Deng and X. Hu, Phys. Rev. B **78**, 245301 (2008).
[29] Ł. Cywiński, W.M. Witzel, and S. Das Sarma, Phys. Rev. Lett. **102**, 057601 (2009).
[30] Ł. Cywiński, W.M. Witzel, and S. Das Sarma, Phys. Rev. B **79**, 245314 (2009).
[31] W.A. Coish, J. Fischer, and D. Loss, Phys. Rev. B **81**, 165315 (2010).
[32] Ł. Cywiński, `arXiv:1009.4466`.
[33] D. Loss and D.P. DiVincenzo, Phys. Rev. A **57**, 120 (1998).
[34] B.E. Kane, Nature **393**, 133 (1998).
[35] D.P. DiVincenzo, D. Bacon, J. Kempe, G. Burkard, and K.B. Whaley, Nature **408**, 339 (2000).
[36] M. Friesen, P. Rugheimer, D.E. Savage, M.G. Lagally, D.W. van der Weide, R. Joynt, and M.A. Eriksson, Phys. Rev. B **67**, 121301(R) (2003).
[37] J.M. Taylor, H.A. Engel, W. Dur, A. Yacoby, C.M. Marcus, P. Zoller, M.D. Lukin, Nature Phys. **1**, 177 (2005).
[38] M. Friesen, A. Biswas, X. Hu, and D. Lidar, Phys. Rev. Lett. **98**, 230503 (2007).
[39] S.I. Erlingsson, Yu.V. Nazarov, and V.I. Fal'ko, Phys. Rev. B **64**, 195306 (2001).
[40] W.A. Coish and D. Loss, Phys. Rev. B **72**, 125337 (2005).
[41] W. Yang and R.B. Liu, Phys. Rev. B **77**, 085302 (2008).
[42] M. Prada, R.H. Blick, and R. Joynt, Phys. Rev. B **77**,

115438 (2008).
[43] X. Hu and S. Das Sarma, Phys. Rev. A **61**, 062301 (2000).
[44] X. Hu and S. Das Sarma, Phys. Rev. Lett. **96**, 100501 (2006).
[45] D. Culcer, X. Hu, and S. Das Sarma, Appl. Phys. Lett. **95**, 073102 (2009).
[46] K. Roszak and P. Machnikowski, Phys. Rev. B **80**, 195315 (2009).
[47] G. Ramon and X. Hu, Phys. Rev. B **81**, 045304 (2010).
[48] G.D. Mahan, *Many-Particle Physics* (Kluwer, New York, 2000).
[49] P. Yu and M. Cardona, *Fundamentals of Semiconductors* (Springer, New York, 2001).
[50] J. Fabian and S. Das Sarma, Phys. Rev. Lett. **81**, 5624 (1998).
[51] J. Fabian and S. Das Sarma, Phys. Rev. Lett. **83**, 1211 (1999).
[52] P. Stano and J. Fabian, Phys. Rev. Lett. **96**, 186602 (2006).
[53] P. Stano and J. Fabian, Phys. Rev. B **74**, 045320 (2006).
[54] J.I. Climente, A. Bertoni, G. Goldoni, M. Rontani, and E. Molinari, Phys. Rev. B **75**, 081303 (2007).
[55] V.N. Golovach, A.V. Khaetskii, and D. Loss, Phys. Rev. B **77**, 045328 (2008).
[56] D. Mozyrsky, S. Kogan, V.N. Gorshkov, and G.P. Berman, Phys. Rev. B **65**, 245213 (2002).
[57] M. Stroscio, *Phonons in Nanostructures* (2000).
[58] *Landolt-Börnstein Numerical Data and Functional Relationships in Science and Technology*, New Series, vol. 17a, page 46 (Springer-Verlag, Berlin, 1982).
[59] L.M. Duan and G.C. Guo, Phys. Rev. A **57**, 737 (1998).
[60] D. Mozyrsky and V. Privman, J. Stat. Phys. **91**, 787 (1998).
[61] B. Krummheuer, V. M. Axt, and T. Kuhn, Phys. Rev. B **65**, 195313 (2002).
[62] A. Vagov, V. M. Axt, and T. Kuhn, Phys. Rev. B **66**, 165312 (2002).
[63] L. Fedichkin and A. Fedorov, Phys. Rev. A **69**, 032311 (2004).
[64] P. Borri, W. Langbein, U. Woggon, V. Stavarache, D. Reuter, and A. D. Wieck, Phys. Rev. **71**, 115328 (2005).
[65] V. M. Axt, P. Machnikowski, and T. Kuhn, Phys. Rev. B **71**, 155305 (2005).
[66] V.N. Stavrou and X. Hu, Phys. Rev. B **72**, 075362 (2005).
[67] B. Krummheuer, V. M. Axt, and T. Kuhn, Phys. Rev. B **72**, 245336 (2005).
[68] T.E. Hodgson, L. Viola, and I. D'Amico, Phys. Rev. A **81**, 062321 (2010).
[69] P. Machnikowski, Phys. Rev. Lett. **96**, 140405 (2006).
[70] P. Meystre and M. Sargent III, *Elements of Quantum Optics* (Springer-Verlag, New York 1991).
[71] A. Huynh, N.D. Lanzillotti-Kimura, B. Jusserand, B. Perrin, A. Fainstein, M.F. Pascual-Winter, E. Peronne, and A. Lemaitre, Phys. Rev. Lett. **97**, 115502 (2006).
[72] G. Rozas, M.F. Pascual Winter, B. Jusserand, A. Fainstein, B. Perrin, E. Semenova, and A. Lemaitre, Phys. Rev. Lett. **102**, 015502 (2009).
[73] C. Herring, Phys. Rev. **95**, 954 (1954).
[74] J.M. Ziman, *Electrons and Phonons* (Oxford University Press, New York, 1960).
[75] D. von der Linde, J. Kuhl, and H. Klingenberg, Phys. Rev. Lett. **44**, 1505 (1980).
[76] B.K. Ridley and R. Gupta, Phys. Rev. B **43**, 4939 (1991).
[77] G. Burkard, D. Loss, and D.P. DiVincenzo, Phys. Rev. B **59**, 2070 (1999).
[78] V.W. Scarola and S. Das Sarma, Phys. Rev. A **71**, 032340 (2005).
[79] Q. Li, L. Cywinski, D. Culcer, X. Hu, and S. Das Sarma, Phys. Rev. B **81**, 085313 (2010).
[80] K. Ono, G. Austing, Y. Tokura, and S. Tarucha, Science **297**, 1313 (2002).